Both RNA-Binding Domains in Heterogenous Nuclear Ribonucleoprotein A1 Contribute toward Single-Stranded-RNA Binding†

Yousif Shamoo, Norzehan Abdul-Manan, Ann M. Patten, Janet K. Crawford, Matthew C. Pellegrini, and Kenneth R. Williams*,‡

Department of Molecular Biophysics and Biochemistry and Howard Hughes Medical Institute, Yale University School of Medicine, 333 Cedar Street, New Haven, Connecticut 06510-8024

Received January 28, 1994; Revised Manuscript Received April 29, 1994®

ABSTRACT: Heterogenous nuclear ribonucleoproteins (hnRNPs) such as hnRNP A1 are tightly associated with heterogenous nuclear RNAs (hnRNAs) within eukaryotic nuclei and are thought to be involved in hnRNA processing and splice site selection. The NH_2-terminal two-thirds of hnRNP A1 contains two 92-amino acid RNA binding domains (RBDs) that are arranged in tandem and are more than 30% homologous with each other. Following this region is a flexible glycine-rich COOH-terminal domain. We have studied the nucleic acid binding properties of the two isolated RBDs (residues 1–92 and 93–184, respectively) and of A1 fragments corresponding to residues 1–184 and 1–196 (i.e., the latter fragment is called UP1) in order to evaluate their relative contributions to A1 binding. We have determined that the individual RBDs of A1 bind poly[r(ϵA)], a fluorescent single-stranded RNA (ssRNA), with a surprisingly low apparent association constant of only 1.5×10^4 M^{-1} (1–92) and 4.5×10^4 M^{-1} (93–184), respectively. We hypothesize that this low affinity represents a basal level of binding that is common to most RBD-containing proteins. Oligonucleotide binding studies suggest the interaction site size for the 93–184 fragment is ~4 nucleotides or less and salt sensitivity studies indicate that only about 27% of the free energy of binding of this RBD derives from ionic interactions. Since the affinity of the 1–184 fragment is at least 10-fold above that of either of its component RBDs, both must contribute to binding. This conclusion is further supported by the increased occluded site size of 1–184 ($n = 14 \pm 2$), as compared to its 93–184 RBD ($n = 6 \pm 1$), and by the biphasic binding that was observed for the UP1:poly(U) interaction at pH 6.0. Our finding that the affinity of the 1–184 fragment is 1000-fold less than the product of the affinities of its 1–92 and 93–184 RBDs is consistent with these domains being joined by a flexible linker. By comparing the affinities of the 1–184 fragment with that for A1, we conclude that together the two RBDs in A1 account for only 53% of the free energy of A1 binding. Comparative binding studies with UP1 demonstrate that the short region spanning residues 185 → 195 represents an important determinant of the binding affinity of A1 and, since this region contains a site of dimethylation, it may provide a mechanism for regulating the affinity of A1 for specific nucleic acid targets.

Heterogenous nuclear ribonucleoproteins (hnRNPs) are abundant proteins that are primarily found in the eukaryotic cell nucleus associated with pre-mRNA transcripts (for recent reviews see Merrill & Williams *et al.*, 1990; Dreyfuss *et al.*, 1993). Heterogeneous nuclear RNAs (hnRNA) are complexed as nascent RNA polymerase II transcripts by at least 20 different proteins (Pinol-Roma *et al.*, 1992). Six of the more abundant proteins that were first identified as being associated with hnRNA migrate on SDS–polyacrylamide gel electrophoresis as three closely spaced doublets that range from about 32 000 to 43 000 in apparent molecular weight. These six proteins were named A1, A2; B1, B2; and C1, C3, respectively (Beyer *et al.*, 1977). In addition to a role in hnRNA packaging and mRNA transport, immunodepletion studies suggest that hnRNPs are also essential for pre-mRNA splicing (Choi *et al.*, 1986; Sierakowska *et al.*, 1986). Finally, several recent studies (Biamonti *et al.*, 1993; Mayeda & Krainer, 1992; Ge & Manley, 1990; Harper & Manley, 1991) suggest that the A1 hnRNP protein may play a direct role in tissue specific and developmental control of gene expression by influencing 5′-splice site selection in pre-mRNAs that contain multiple 5′-splice sites.

The A1 hnRNP is the best characterized of the hnRNP proteins and consists of 319 amino acids (34 kDa) (Cobianchi *et al.*, 1986). A1 binds tightly and cooperatively to single-stranded nucleic acids with a 100-fold or greater preference (in 0.15 M NaCl) for single-stranded RNA as compared to single or double-stranded DNA (Nadler *et al.*, 1991). cDNA sequences of hnRNP A1 from rat (Cobianchi *et al.*, 1986) have shown that residues 1–195 of A1 are identical to UP1 isolated from calf thymus (Williams *et al.*, 1985). UP1 is presumed to result from proteolysis that occurs *in vitro* following cell disruption (Valentini, *et al.*, 1985).

Analysis of the primary structure of A1 (Merrill *et al.*, 1986) and limited proteolysis studies (Kumar *et al.*, 1986) both suggested that this hnRNP protein contains two primary domains, the 1–195 UP1 region and the glycine-rich, 196–319 COOH-terminal domain (see Figure 1). Binding studies on UP1 that was either isolated from mammalian sources or produced via limited proteolysis of recombinant A1 demonstrated that UP1 binds single-stranded RNA (ssRNA) or single-stranded DNA (ssDNA) non-cooperatively and that (in <25 mM NaCl) it has an approximately 10-fold preference for binding ssRNA as compared to ssDNA and about a 350-fold preference for ssDNA as compared to dsDNA (Cobianchi *et al.*, 1988; Nadler *et al.*, 1991). Further proteolysis of UP1 revealed two 92-amino acid subdomains that bind ssDNA (Merrill *et al.*, 1986). These two domains are homologous to

† Supported by NIGMS Grant GM31539 to K.R.W.
‡ Howard Hughes Medical Institute.
® Abstract published in *Advance ACS Abstracts,* June 15, 1994.

0006-2960/94/0433-8272$04.50/0

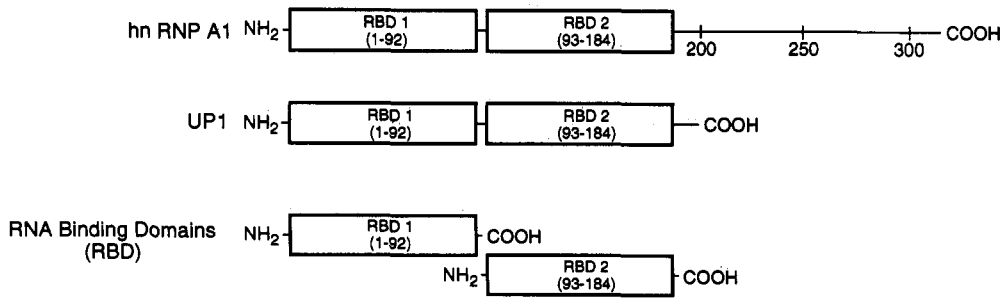

FIGURE 1: Schematic representation of the hnRNP A1 protein. RBD 1 extends from residues 1–92, RBD 2 from 93–184, and residues 196–319 make up a flexible glycine-rich C-terminus. UP1 consists of residues 1–195 and thus contains both RBDs as well as a short stretch of 11 residues containing two arginine residues.

each other such that when residues 3–93 are aligned with 94–194, 32% of the amino acid residues are identical (Merrill *et al.*, 1986). On the basis of the high degree of conservation of basic and aromatic residues in these domains (62% and 80%, respectively), these two internal repeats were postulated to contain two independent nucleic acid binding sites (Merrill *et al.*, 1986). Subsequently, homologous, ~90-residue RNA binding domains were found in the yeast poly(A) binding protein (Adam *et al.*, 1986) and now in more than 30 other eukaryotic RNA binding proteins. This ~90-residue domain has been referred to as the RNA-binding domain (RBD, Dreyfuss *et al.*, 1988) or the RNA recognition motif (RRM, Query *et al.*, 1989) and proteins have been found that have as few as one (type C hnRNP) to as many as four (nucleolin and the poly(A) binding protein) of these domains (Bandziulis *et al.* 1989; Merrill & Williams, 1990; Kenan *et al.*, 1991).

Within each of the 90-amino acid A1 RNA-binding domains, two short sequences spanning residues 54–61, R-G-F-G-F-V-T-Y (RNP-1), and 15–20, L-F-I-G-G-L (RNP-2), were particularly well conserved among this family of eukaryotic ssRNA binding proteins (Dreyfuss *et al.*, 1988). Photochemical cross-linking of A1 to oligo $p(dT)_8$ demonstrated that one phenylalanine residue within each of these stretches of sequence (residues 58 and 16, respectively) is at the A1:nucleic acid interface (Merrill *et al.*, 1988). A recent crystal structure of the related small nuclear ribonucleoprotein U1A from the eukaryotic spliceosome demonstrates that the two corresponding residues in the U1A RBD (tyrosine 13 and phenylalanine 56) are actually located next to each other on two antiparallel β-strands that are in the center of a four-stranded β-pleated sheet that was proposed to form much of the nucleic acid binding surface of the RBD (Nagai *et al.*, 1990). *In vitro* mutagenesis studies on the U1A RBD (Jessen *et al.*, 1991) and multidimensional NMR studies on the NH_2-terminal 93 residues of hnRNP C (Görlach *et al.*, 1992) both confirm that this four-stranded β-pleated sheet is directly involved in nucleic acid binding.

The COOH-terminal domain of A1 has several unique features that differentiate it strongly from the NH_2-terminal two-thirds of the protein. The 124 residues at the COOH-terminus of A1 have an unusually high glycine content (45%) and a reasonably well conserved repeat sequence, G-N-F/Y-G-G-S/G-R-G, that provides a regular spacing of flexible, aromatic, and positively charged residues (Wilson *et al.*, 1987, Cobianchi, *et al.*, 1988). Physicochemical studies have demonstrated that the COOH-terminal region is entirely responsible for the A1:A1 protein:protein interactions that result in A1 aggregation in solution and cooperative interactions between adjacent A1 molecules bound to a nucleic acid lattice (Cobianchi *et al.*, 1988; Kumar *et al.*, 1990; Nadler *et al.*, 1991; Casas-Finet *et al.*, 1993). In addition, the COOH-terminal domain also interacts directly with the bound nucleic acid (Cobianchi *et al.*, 1988; Kumar *et al.*, 1990; Nadler *et al.*, 1991; Casas-Finet *et al.*, 1993). Finally, the strand-annealing activity of A1 is localized in the COOH-terminal domain (Kumar & Wilson, 1990; Munroe & Dong, 1992) and this activity can be modulated by phosphorylation of a serine residue located within this domain (Cobianchi *et al.*, 1993).

We have extended the analysis of the NH_2-terminal 1–195 residue or UP1 domain of A1 to examine the contribution of the individual 92 amino acid RBDs (1–92 and 93–184) to UP1 and A1 binding to single-stranded nucleic acids. In addition, we have further dissected the NH_2-terminal 1–92 domain into two smaller peptides to try to examine the potential contribution of the two individual RBD consensus sequences in this domain toward ssRNA binding and specificity. Using a variety of physicochemical approaches we have characterized the structures and nucleic acid binding affinities of UP1 fragments corresponding to residues 4–49, 50–93, 1–92, 93–184, 1–184, and 1–195. Our results suggest that, as expected from the NMR and crystallographic studies, the individual RBDs are well-ordered semi-independent structural domains capable of binding ssRNA preferentially over ssDNA. Once the individual RBDs for A1 had been characterized and their association constants to ssRNA measured, it became apparent that both RBDs were probably required to attain the much higher association constants determined for the 1–184 or 1–195 (UP1) species. We hypothesize that the "nonspecific" affinity of the A1 RBD is representative of the "basal" level of binding energy that is probably shared by most, if not all, RBDs. The results of our studies provide a starting point for modeling basal RBD:ssRNA affinities and contribute to our general understanding of single-stranded nucleic acid binding.

MATERIALS AND METHODS

Cloning and Overexpression of the 1–195 Domain (UP1). Plasmid pEX11 containing the gene for A1 was the generous gift of S. H. Wilson (Cobianchi *et al.*, 1988). pEX11 was digested with the restriction endonuclease *Xmn*I to release a 545-bp fragment (47–592) that included most of the UP1 sequences. The 5′- and 3′-ends of UP1 were reconstructed using two sets of oligodeoxynucleotide linkers. The 5′-linker restored the 46 nucleotides at the 5′-end of the gene and contained a ribosome binding site modeled on that used by *Escherichia coli* SSB and used successfully for the overexpression of bacteriophage T4 gene 32 (Shamoo *et al.*, 1986). The 5′-linker also contained a convenient restriction site for *Eco*RI just 5′ of the ribosome binding site. The 3′-linker added the translation stop codon UAA at position 592 with a convenient *Bam*H1 site 11 nucleotides 3′ of the stop. The purified A1 *Xmn*I fragment, two sets of linkers, and *Eco*RI/*Bam*H1 digested pUC18 were ligated using T4 DNA ligase and transformed into *E. coli* DH5α (Sambrook *et al.*, 1989).

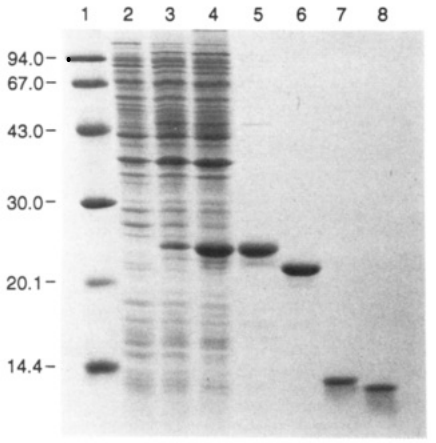

FIGURE 2: Time course for the overexpression of recombinant UP1 and examples of UP1 subdomains made via partial trypsin proteolysis: lane 1, molecular weight markers; lanes 2–4, time course of recombinant UP1 expression from *E. coli* BL21DE3 containing plasmid pYS45 induced with IPTG at 0, 4, and 8 h, respectively; lane 5, purified UP1; lane 6, purified 1–184 fragment; lane 7, 1–92 fragment (RBD 1); lane 8, 93–184 fragment (RBD 2). Construction of plasmid pYS45 and purification schemes for the isolation of each subdomain are more fully described in Materials and Methods.

Clones containing the expected ~0.6-kb *Eco*RI/*Bam*HI insert were sequenced prior to subcloning into the *Eco*RI/*Bam*HI sites of the T7 expression vector p7A7W (the gift of T.C. Lin) and transforming into *E. coli* BL21DE3 as pYS45 (Sambrook *et al.*, 1989).

E. coli BL21DE3 carrying pYS45 (encoding residues 1–195 of A1) was grown at 37 °C to an A_{590} of 0.5 in LB media with 0.1 mg/mL ampicillin prior to induction with isopropyl thio-β-D-galactoside (IPTG) at a final concentration of 0.65 mM (Sambrook *et al.*, 1989). Cells were allowed to induce for 8–16 h before harvesting. Densitometry of 15% acrylamide SDS gels indicated that, as expected, a protein of about 22 kDa had been induced and this band made up about 10% of the total soluble cellular protein (Figure 2).

Purification of UP1 (1–195), 1–184, 1–92, and 93–184 Peptides. Cells were lysed by sonication and cleared by centrifugation prior to being loaded onto a DE52 column (4.5 cm × 20 cm) equilibrated in 50 mM NaCl, 10 mM Tris 8.0, 0.1 mM EDTA, 1 mM DTT, 0.1 mM PMSF, and 10% (v/v) glycerol (buffer A). The DE52 column was eluted with a linear gradient from 0.05 to 1 M NaCl with the recombinant UP1 eluting at 100–200 mM NaCl. The partially purified UP1 was dialyzed back into buffer A, loaded onto a ssDNA cellulose column (2.5 × 20 cm), and then eluted with a linear gradient extending from 0.05 M to 1 M NaCl. The purified UP1 eluted at 80–180 mM NaCl and was quantitated by amino acid analysis. In general, yields of 8–10 mg of UP1/g wet weight of cells were obtained by this expression and purification scheme. On the basis of SDS–PAGE, the resulting UP1 was nearly homogenous (Figure 2).

Fragments 1–92 and 93–184 were made by digestion of UP1 with *Staphylococcus aureus* V8 protease (Pierce) at 37 °C that had been covalently attached to Bio-Rad Affi-gel 10 resin following the manufacturer's recommended procedures. Since the degree of cross-linking of protease V8 to Affigel 10 was somewhat variable, analytical digests were performed and examined by SDS–PAGE in order to optimize the time and ratio of resin to UP1. The immobilized protease was removed by filtration and reused. The filtered solutions containing the UP1 fragments were treated with 0.2 mM diisopropyl fluorophosphate (DFP, diisopropyl phosphorofluoridate). In addition, 0.1 mM PMSF was included in all subsequent buffers. The digest was dialyzed versus 5 mM phosphate, pH 6.0, 0.1 mM PMSF, 1 mM DTT, and 3 mM sodium azide (buffer B) prior to loading onto a Mono-S column (2.5 × 20 cm) equilibrated at 20 °C in buffer B. The Mono-S column was eluted with a linear salt gradient extending from 0 to 1 M NaCl with the 1–92 fragment eluting late in the flow through and at the start of the gradient and the 93–184 fragment eluting at ca. 100 mM NaCl. Appropriate fractions were pooled and concentrated using an Amicon ultrafiltration unit prior to quantitation by amino acid analysis. SDS–PAGE indicated that the resulting fragments were nearly homogenous (Figure 2).

In order to make the 1–184 partial proteolysis fragment, UP1 was digested with free *S. aureus* V8 protease at a ratio of 1:150 (w/w, V8/UP1) at 25 °C for 30 min. As demonstrated by SDS–PAGE (Figure 2), the 1–184 fragment was readily purified from residual UP1 and V8 protease by ssDNA cellulose chromatography under the conditions described above.

Synthesis of the 4–49 and 50–93 Peptides. The 4–49 and 50–93 residue peptides were synthesized at the W. M. Keck Foundation Biotechnology Resource Laboratory at Yale University. Analytical HPLC showed that the purity of the synthesized peptides was >95% and FAB mass spectrometry verified that the peptides had the expected mass (data not shown).

Nucleic Acids. Oligonucleotides were made at the W. M. Keck Foundation Biotechnology Resource *Laboratory* at Yale University. Poly[r(A)], -[d(A)], and -[r(U)] were obtained from Pharmacia. Poly[d(A)] and -[r(A)] were ethenylated and quantitated as described by Nadler *et al.* (1991).

Circular Dichroism. An Aviv Model 60DS spectropolarimeter was used to collect data over the range of 300–200 nm at 0.5-nm intervals in a 0.1-cm pathlength cuvette. The samples were exchanged into either 20 mM Tris 8.0 or 20 mM phosphate, pH 6.0, as indicated, and protein concentrations, which ranged from 12 to 25 μM, were determined by amino acid analysis. The data from five repeat scans were used to fit the spectra as a polynomial function. All spectra were corrected for contribution from the buffer. Estimates of secondary structure were made using the Prosec algorithm developed by Aviv as described by Chang *et al.* (1978).

Fluorescence Spectroscopy. Fluorescence titrations were carried out on an SLM 8000C spectrofluorometer interfaced to an HP Vectra microcomputer. Titrations were performed in a volume of 2 mL in temperature-regulated and continuously stirred quartz cuvettes. An average of three 10-s acquisitions were used for each data point. "Forward" titrations with ethenylated nucleic acids were carried out with an excitation wavelength of 315 nm and an emission wavelength of 400 nm. Corrections were made for dilution effects resulting from the sequential addition of protein and for background fluorescence. "Reverse" titrations were carried out with an excitation wavelength of 280 nm and an emission wavelength of 325 nm. Reverse titrations were corrected for background fluorescence, dilution, photobleaching, and inner filter effects due to the addition of polynucleotides. Inner filter corrections were calculated from a third-order regression analysis of curves obtained from titrating *N*-acetyltryptophanamide with the appropriate polynucleotide. Both forward and reverse titrations used an 8-nm bandpass for the emission and excitation wavelengths.

The occluded site size, *n* (the number of nucleotides covered by a protein molecule), for the peptides was determined using titrations performed under stoichiometric conditions, with *n*

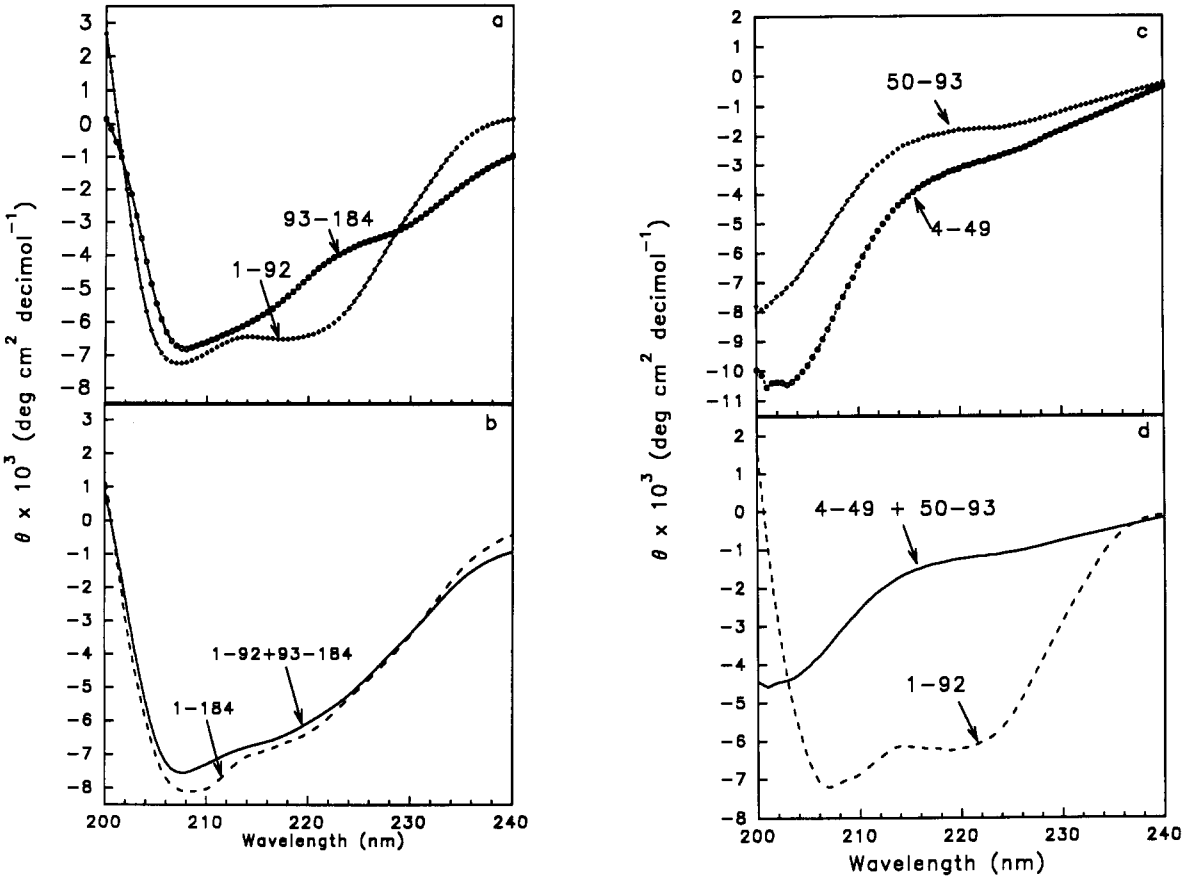

FIGURE 3: Circular dichroism studies on the 1–184 fragment, its constituent RBDs and synthetic peptides derived from the 1–92 sequence: (a) the CD spectra obtained for each of the isolated 1–92 and 93–184 RBDs, (b) compares the actual CD spectra for the 1–184 fragment to a calculated spectra that was obtained by adding together the data shown in part a for the 1–92 and 93–184 fragments, (c) the spectra obtained for the two synthetic peptides containing residues 4–49 and 50–93, (d) compares the actual CD spectra for the 1–92 fragment derived by partial proteolysis from UP1 (1–196) to that obtained by adding the 4–49 and 50–93 spectra. Sample preparation and data analysis are discussed more fully in Materials and Methods.

being shown to be invariant with the poly[r(ϵA)] concentration. Binding constants for the titrations with poly[r(ϵA)] were estimated using a visual curve fitting and statistical analysis procedure based on the closed expression derived by McGhee and von Hippel (1974). Using a fixed site size determined as described above, K_{int} and ω were independently varied to obtain the best visual match of the theoretical curve (generated using eq 15 of McGhee & Von Hippel, 1974) to the experimental data. In those instances where titrations did not reach saturation, the maximum fluorescence value was also varied. Having obtained approximate K_{int} and ω values by this visual curve-fitting procedure, these parameters were further refined by carrying out a nonlinear least squares analysis as described by McSwiggen *et al.* (1988) and Kowalczykowski *et al.* (1986).

The interaction site size for the 93–184 RBD was estimated by carrying out titrations with a series of oligonucleotides, $r(\epsilon A)_x$, where x was equal to 4, 6, 8, 10, and 12. By using a "double reciprocal" plot of $(1/\Delta F$ versus $1/[\text{peptide}]_{free})$, the apparent affinities of the oligos for 93–184 can be determined using the formula $K_{app} = 1/(\text{slope} \times \Delta F_{max})$ where ΔF_{max} is equal to the y-intercept and the slope is obtained via linear regression. As long as the increased number of bases can interact effectively with the peptide, there will be a significant increase in K_{app} as the length of the oligo is increased. Hence, one method for estimating the interaction site size is to determine the point at which lengthening the oligonucleotide does not result in any further increase in apparent affinity. The only caveat to this approach is that a small correction has to be made for the expected increase in affinity that is due to statistical shuffling as the oligonucleotide is lengthened beyond the occluded site size (Kelly *et al.* 1976).

RESULTS

Circular Dichroism Studies Suggest That Cleavage of the 1–184 Fragment into Its Constituent RBDs Does Not Alter Their Overall Secondary Structures. Of particular importance to this study is the finding that the CD spectra of the 1–184 fragment is almost exactly equal to the sum of the spectra of its two RBDs (Figure 3b). Hence, it appears that cleavage of the 1–184 fragment into its two RBDs has not resulted in any major alteration in the overall secondary structures of these domains. Similarly, since the CD spectra for the 1–184 and 1–195 (UP1) fragments were essentially identical (data not shown), removal of residues 185–195 from UP1 also does not result in any major changes in secondary structure. Similar CD spectra as those shown in Figure 3a,b, which were obtained at pH 8, were also obtained at pH 6 for 1–184 and its two fragments. This is an important finding because the solution structure of the type C RBD was determined at acid pH (i.e., pH 5.5; Wittekind *et al.*, 1992). As shown in Figure 3a, there are significant differences in the 215–240-nm region of the circular dichroism (CD) spectra of the two UP1 RBDs as determined from secondary structure analysis of the CD data (Table 1). These differences may be attributable primarily to the 1–92 fragment having significantly more β-sheet-like structure and less random coil than the 93–184 fragment. As seen in Table 1, hnRNP C and

Table 1: Estimated Secondary Structure of UP1 and Its Fragments Based on Circular Dichroism Spectra

protein	% α-helix	% β-sheet	% turn	% coil
UP1/1–195	17	30	19	35
1–184	18	29	20	32
1–92	14	46	13	27
93–184	18	21	28	33
4–49	0.0	23	26	33
50–93	0.0	26	26	47
hnRNP C[a]	23	22	11	45
snRNP U1/A[b]	28	31	10	35

[a] Calculated from structure of Wittekind *et al.* (1992). [b] Calculated from structure of Nagai *et al.* (1990).

snRNP U1A also show pronounced differences in overall β-sheet content although their overall folds are largely identical (Nagai *et al.*, 1990; Hoffman *et al.*, 1991).

In contrast to the apparent additivity of the CD spectra of the two constituent domains of 1–184, the sum of the CD spectra of synthetic peptides corresponding to the two halves of the 1–93 domain did not approximate the spectra for the intact RBD (Figure 3c,d). As indicated in Table 1, the two synthetic peptides lack all of the α-helical and much of the β-sheet structure that is predicted for the native 1–92 domain.

Both RBDs in UP1 Contribute toward Binding. The fluorescence binding studies shown in Figure 4a, which were carried out in 20 mM Tris, pH 8.0, indicate that while UP1 binds stoichiometrically under these conditions, the 1–184, 1–92, and 93–184 peptides all bind much more weakly. Surprisingly, there was a 100-fold reduction in apparent affinity observed upon going from UP1, which contains residues 1–195, to 1–184 (Table 2). In comparison, there was only a further 12-36-fold decrease in affinity at pH 8 upon removing an entire 92-residue RBD domain from the 1–184 fragment (Table 2). Nonetheless, the latter strongly suggests that both RBDs in the 1–184 fragment contribute to binding.

Since the native secondary structure of 1–92 is clearly not retained in its two synthetic peptide analogues (Figure 3d), it was surprising to find that the 50–93 fragment actually binds 5-fold more tightly than the 1–92 fragment does to poly[r(εA)]. This result parallels similar data on the corresponding peptide analogues from an RBD in the yeast poly A binding protein (Nadler *et al.*, 1992). As in the latter instance, we hypothesize that binding of the 50–93 fragment to poly[r(εA)] is a function of its amino acid composition rather than of its amino acid sequence and higher order structure.

Table 2: Binding of UP1 and Its Fragments to Poly[r(εA)]

protein	pH 6 net charge[a]	pH 6 n^b	pH 6 K_{app}^d (M^{-1})	pH 8 net charge[a]	pH 8 n^b	pH 8 K_{app} (M^{-1})
1–195 (UP1)	+9	15 ± 1	2.2×10^8	+1	10 ± 1	6.6×10^7
1–184	+7	14 ± 2	9.1×10^6	−1	14 ± 2	5.4×10^5
1–92	+2	(6)	2.8×10^4	0	(6)	1.5×10^4
93–184	+5	6 ± 1	3.8×10^5	−1	(6)	4.5×10^4
4–49				−4		ND[c]
50–93				+2	4	7.8×10^4

[a] All histidines are assumed to be fully protonated at pH 6. [b] *n* values in parentheses represents an assumed value, as opposed to being experimentally determined. [c] ND indicates that no detectable binding was observed. [d] Since all of the proteins in Table 2 had cooperativity parameters that were ~1, the K_{app} is equal to the K_{int} (McGhee & von Hippel, 1974).

Presumably as a result of their greater net positive charge at pH 6, UP1 and its fragments all bound more tightly to poly[r(εA)] at pH 6 than at pH 8 (Figure 4b, Table 2). The affinity of the 93–184 fragment was sufficiently high at pH 6 that it was possible to directly determine its occluded site size, which was found to be approximately 6 nucleotides (Table 2). This value is slightly less than half of the site size of 14 that was determined at pH 6 for the 1–184 fragment. Although the relatively weak binding of the 1–92 and 93–184 fragments at pH 8 precluded a direct determination of their site sizes, the value of 6 nucleotides was consistent with curve fitting. UP1 is unusual in that the apparent site size decreases from ~15 to ~10 as the pH is increased from 6 to 8 (Table 2). This latter estimate is just slightly larger than the previously reported value of ~8 nucleotides (Cobianchi *et al.*, 1988; Nadler *et al.*, 1991; Casas-Finet *et al.*, 1991). Another unusual finding with regard to site size is that at pH 8, the 1–184 fragment appears to have a significantly larger apparent site size than the 1–195 fragment from which it was derived (Table 2). Together, these data suggest that the topological arrangement of the two RBDs in UP1 with respect to the nucleic acid may be altered by either removing residues 185–195 or by substantially decreasing its net positive charge via an increase in pH.

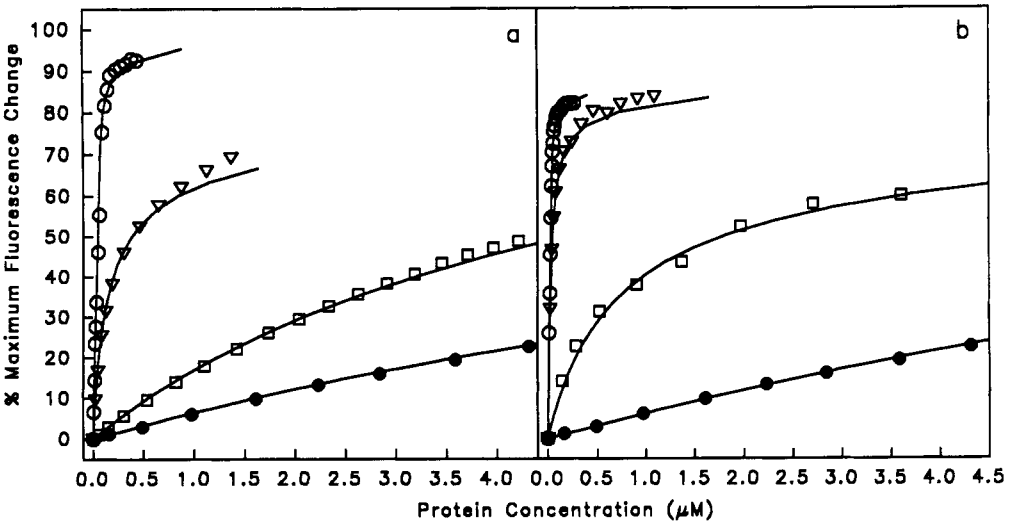

FIGURE 4: Fluorescence titrations of poly[r(εA)] with UP1 and subdomains. Parts a and b show the binding of UP1 (open circles), 1–184 (inverted triangles), 1–92 (filled circles), and 93–184 (open squares) to 1 μM poly[r(εA)] in either 20 mM Tris, pH 8.0, (a) or 20 mM phosphate, pH 6.0 (b). The solid lines are theoretical best-fit curves generated as described in Materials and Methods.

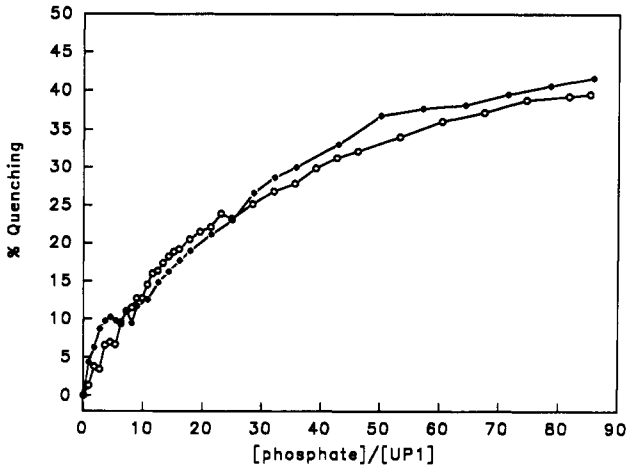

FIGURE 5: "Reverse" titrations of UP1 to poly[r(U)] in 20 mM, Tris 8.0 (open circles), or 20 mM phosphate, pH 6.0 (filled circles). 5 μM UP1 was titrated with increasing amounts of poly[r(U)] and the intrinsic protein fluorescence was monitored at 325 nm at 25 °C. Concentrations of poly[r(U)] are given as micromolar phosphate/micromolar UP1. Conditions for data measurement and analysis are given in Materials and Methods.

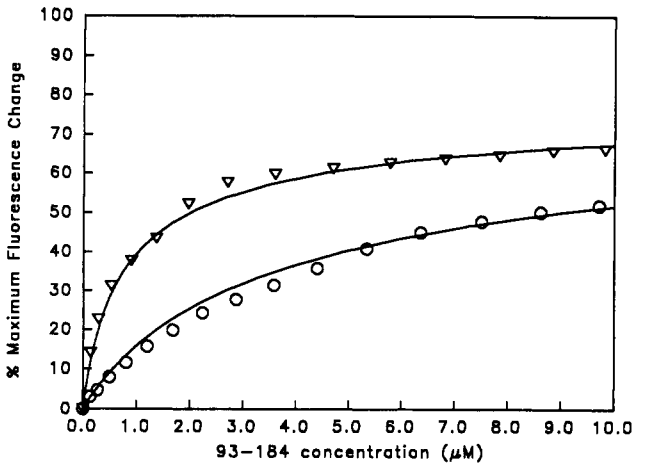

FIGURE 6: Fluorescence titrations of poly[r(εA)] and poly[d(εA)] with the 93–184 fragment. Starting polynucleotide concentrations were 1 μM phosphate. Titrations were carried out in 20 mM phosphate, pH 6.0, at 25 °C. Titration data for poly[r(εA)] (inverted triangles) and poly[d(εA)] (open circles) are indicated and the solid lines are theoretical best-fit curves generated as described in the Materials and Methods.

Table 3: Binding of the A1(93–184) Fragment to $r(\epsilon A)_x$ Oligonucleotides at pH 6

oligo	K_{app}[a] average	K_{app}[a] predicted for $m = 4$[b]
$r(\epsilon A)_4$	$2.0 \pm 0.9 \times 10^4$	
$r(\epsilon A)_6$	$2.9 \pm 2.5 \times 10^4$	6.0×10^4
$r(\epsilon A)_8$	$4.0 \pm 1.5 \times 10^4$	1.0×10^5
$r(\epsilon A)_{10}$	$1.3 \pm 4.0 \times 10^4$	1.4×10^5
$r(\epsilon A)_{12}$	$3.3 \pm 3.3 \times 10^5$	1.8×10^5

[a] K_{app} have been calculated on the basis of the molar [oligo] and a maximal fluorescence enhancement of 200–250%; for additional details on these calculations see Materials and Methods. [b] Based on the method of Kelly et al. (1976) where $K_l = (l - m + 1)K_m$ where "l" is the length of the oligonucleotide and m is the actual interaction site size.

UP1 Binding to Poly(U) at pH 8.0 and 6.0. As shown in Figure 5, binding isotherms for UP1 undergo a subtle but significant change in curve shape upon decreasing the pH from 8 to 6. At pH 6, the initial slope of the curve is noticeably biphasic whereas at pH 8 the curve appears to be monotonic. The former suggests that at pH 6 the two RBDs in UP1 bind independently and that one of the RBDs has a significantly higher affinity than the other one does for poly(U). On the basis of the data in Figure 5, UP1 has an affinity of about 1.3×10^5 M^{-1} for poly(U). This value is similar to the previously reported affinity of 4.7×10^5 M^{-1} (Nadler *et al.*, 1991) and indicates that UP1 binds poly[r(εA)] at least 2 orders of magnitude more tightly than it does poly(U).

Oligonucleotide Binding Studies Suggest the Interaction Site Size for the 93–184 RBD Domain Is ~4 Nucleotides or Less. Although near stoichiometric titrations with poly[r(εA)] provided an estimate of six nucleotides for the occluded site size of the 93–184 fragment, the actual interaction site size may well be less than this value. In order to approach this question, binding studies were carried out with a series of ethenylated oligonucleotides of the structure $[r(\epsilon A)]_x$ where x was equal to 4, 6, 8, 10, and 12. As shown in Table 3, there was only a ca. 15-fold increase in the apparent affinity for the 93–184 fragment on going from $[r(\epsilon A)]_4$ to $[r(\epsilon A)]_{12}$. Although significant, this relatively small increase in affinity can (within the accuracy of the values reported in Table 3) be fully attributed to entropic factors resulting from the fact that once the oligonucleotide is extended beyond the interaction site size, multiple (albeit equivalent) binding sites become available for the 93–184 fragment. Hence, the intrinsic free energy of oligonucleotide binding to the 93–184 fragment appears to be constant throughout this series of oligonucleotides. This result suggests that the actual interaction site size for the 93–184 fragment is no longer than about 4 nucleotides and that, in agreement with our poly[r(εA)] studies, binding of the 93–184 fragment is non-cooperative. The finding that at pH 6 the affinity of the 93–184 fragment for $[r(\epsilon A)]_6$ (Table 3) is ca. 10-fold less than that for poly[r(εA)] (Table 2) suggests that $[r(\epsilon A)]_6$ does not exactly mimic the interaction of 93–184 with a longer polynucloetide lattice. This difference may partially result from the fact that while $[r(\epsilon A)]_6$ has only five phosphates (ie., it was synthesized without a 5′-phosphate), a 6-mer located within poly[r(εA)] would have six phosphates and thus an overall greater negative charge density. Alternatively, the difference may be attributable to the greater mobility or less inherent stacking of the nucleotides at the ends of a relatively short oligonucleotide as compared to the more restricted structure that would probably be imposed on a 6-mer that was located within the context of a polynucleotide.

93–184 RBD Has Higher Affinity for RNA versus DNA. In order to determine whether the 93–184 fragment possesses the same 10-fold preference as UP1 does for ssRNA over ssDNA (Nadler *et al.*, 1991), we determined the affinities of this fragment for poly[r(εA)] versus poly[d(εA)] at pH 6. As shown in Figure 6, 93–184 binding to poly[d(εA)] ($K_{app} = 4.5 \times 10^4$ M^{-1}) is about 8-fold weaker than to poly[r(εA)] (3.8×10^5 M^{-1}). Although the difference in affinity of the 93–184 domain for ssRNA versus ssDNA is relatively small, it nonetheless indicates that this single RBD retains specificity for binding RNA.

Most of the Overall Free Energy of Binding of the 93–184 RBD Appears To Derive from Nonelectrostatic Interactions. Since electrostatic interactions often make large contributions to the overall free energy of protein binding to nucleic acids, the affinity of UP1 and its 1–184 and 93–184 fragments for poly[r(εA)] was determined over a range of salt concentrations in order to evaluate the relative importance of ionic interactions to binding. Record *et al.* (1976) have shown that the slope of a log K_{app} versus log [NaCl] plot can be used to evaluate the maximum number of ionic interactions that could be

Table 4: Summary of Binding Data from Salt Sensitivity Studies of UP1 and Its Fragments

protein	pH	net charge	slope from log–log plot	predicted maximum number of electrostatic interactions[a]	% of electrostatic contribution to binding free energy at 10 mM NaCl
1–195 (UP1)	8	+1	–2.9[b]	4.1	73
1–184	8	–1	–0.9	1.3	33
	6	+7	–1.7	2.5	49
93–184	6	+5	–0.7	1.0	27
50–93	6	+2	–0.5	0.7	18

[a] The value of 0.71 from the slope of a log–log plot represents approximately one ionic interaction as estimated by Record *et al.* (1978). [b] From Nadler *et al.* (1991).

involved in binding. As shown in Table 4, removing residues 185–195 from UP1 to form the 1–184 fragment greatly reduces the salt sensitivity of binding to poly[r(ϵA)]. Hence, whereas UP1 binding at pH 8 appears to involve a maximum of four ionic interactions, 1–184 binding involves a maximum of one to two interactions (Table 4). Taken together with the sequence of residues 185–195 (Met-Ala-Ser-Ala-Ser-Ser-Ser-Gln-Arg-Gly-Arg-Ser), it appears likely that the loss of the two arginine residues in this stretch of sequence accounts for much of the ~100-fold decrease in affinity (at pH 8) that accompanies removal of this short peptide from UP1. As shown in Figure 7a, decreasing the pH from 8 to 6 significantly increases the salt dependence of 1–184 binding such that we estimate that at least one additional ionic interaction may be involved in binding at the lower pH (Table 4). These data suggest that at least one of the eight histidines in the 1–184 fragment may be protonated upon decreasing the pH to 6 and this protonation may enable an additional ionic interaction to occur with the phosphodiester backbone of the nucleic acid lattice. The latter may account for the 17-fold increase in affinity that was seen for the 1–184 fragment as the pH was lowered from 8 to 6 (Table 2). By extrapolating to 1 M salt, where the ionic contribution to binding its negligible (Record *et al.*, 1976), it is possible to estimate the contribution of ionic interactions to the overall free energy of binding. Using this approach, we estimate that in 10 mM NaCl, the electrostatic contribution to the overall free energy of 1–184 binding increases from about 33% to 49% as the pH is decreased from 8 to 6.

On the basis of the data shown in Figure 7b, binding of the 93–184 fragment is even less salt sensitive than that of the 1–184 fragment. In fact, we estimate that, even at pH 6, no more than a single ionic interaction is involved in the binding of the 93–184 fragment to poly[r(ϵA)] (Table 4). In 10 mM NaCl, we estimate that ca. 27% of the free energy of binding of the 93–184 fragment derives from ionic interactions.

DISCUSSION

Despite the fact that the RBD has now been found in more than 30 different eukaryotic RNA binding proteins (Dreyfuss *et al.*, 1988; Bandziulis *et al.*, 1989; Kenan *et al.*, 1991), relatively little has been published about its equilibrium binding properties. Although apparent binding affinities have been reported for the interaction of a few RBDs with specific RNA targets (Sachs *et al.*, 1987; Jessen *et al.*, 1991; Zamore *et al.*, 1992), little has been established concerning the energetics of isolated RBD binding to "nonspecific" targets. The RBDs from the type A and C hnRNP proteins (i.e., see following paper in this issue) provide ideal prototypes for addressing this need as these hnRNP proteins are among the major

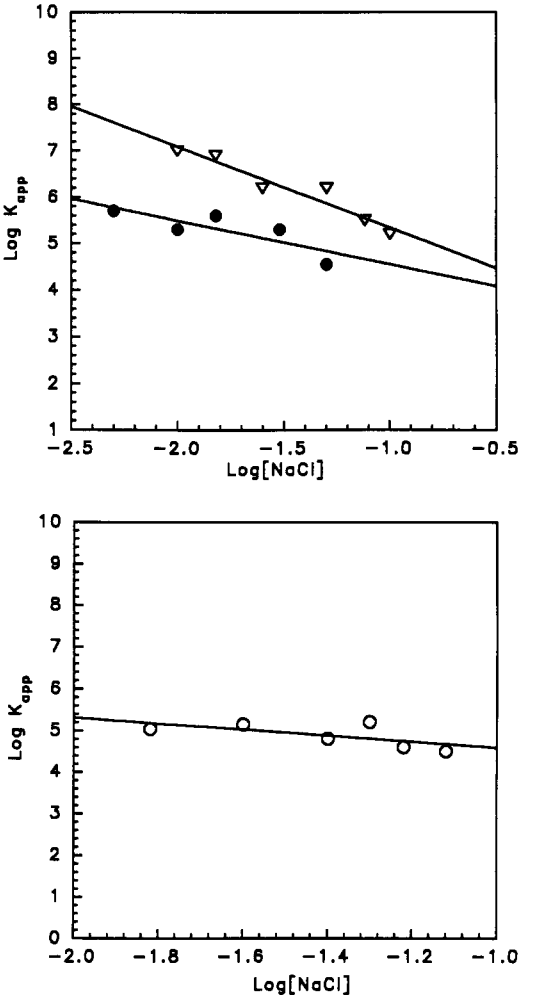

FIGURE 7: (a, top) Effect of NaCl concentration on the affinity of the 1–184 fragment for poly[r(ϵA)]. Association constants were determined from titrations carried out in 20 mM phosphate, pH 6.0, or 20 mM Tris, pH 8.0, with varying concentrations of NaCl at 25 °C. The slopes and *y*-intercepts from a linear least squares fit of the log–log plots are as follows: at pH 8.0 (closed circles), slope = –0.9 and *y*-intercept = 3.7; at pH 6.0 (open triangles), slope = –1.7 and *y*-intercept = 3.6. (b, bottom) Effect of NaCl concentration on the affinity of 93–184 fragment at pH 6.0 for poly[r(ϵA)]. The slope and the *y*-intercept from a linear least squares fit of the log–log plot are –0.7 and 3.9, respectively.

hnRNP proteins that are assumed to bind to all pre-mRNA immediately following transcription (Dreyfuss *et al.*, 1993). Since the type A hnRNP contains two tandemly arranged RBDs, this protein is of further interest from the standpoint of examining the individual contribution of multiple RBDs toward overall nucleic acid binding affinity. Thus, the type A and C hnRNP proteins, in particular, provide an especially good opportunity to evaluate the non-sequence-dependent binding characteristics of isolated RBDs.

One of the most interesting findings that initially arose from these studies was the surprisingly large decrease in RNA affinity that accompanied removal of only 11 amino acid residues (i.e., residues 185–195) from the COOH-terminus of the UP1 protein. Hence, at pH 8, the affinity of 1–184 is more than 100-fold lower than that of UP1 (1–195) for poly-[r(ϵA)]. The corresponding decrease in salt sensitivity suggests strongly that most of this decrease in affinity results from the loss of ionic interactions involving arginines 193 and 195. The latter is particularly intriguing because arginine 193 has been shown to be dimethylated in calf thymus UP1 (Williams *et al.*, 1985). Calnan *et al.* (1991) have suggested that

dimethylation of arginine residues might provide a general mechanism for modulating the specific binding affinities of many RNA binding proteins. That is, dimethylation would be expected to block the hydrogen-bonding interactions that are thought to occur in "arginine forks" and that account for specific target recognition but would not alter the charge of the side chain. Hence, nonspecific ionic interactions with the phosphodiester backbone of nucleic acids would not be expected to be significantly decreased by dimethylation (Calnan *et al.*, 1991). It is intriguing, therefore, to speculate that dimethylation might modulate the ability of the A1 hnRNP to recognize 3′-splice sites (Swanson and Dreyfuss, 1988; Buvoli et al., 1990).

Once the affinity of the 1–184 fragment for poly[r(ϵA)] was determined, the question of the relative contributions of the RBD-containing NH_2-terminal (residues 1–184) and glycine-rich COOH-terminal (residue 185–319) domains of A1 could be addressed directly. On the basis of the data in Table 4, the calculated apparent affinity of the 1–184 fragment at pH 8 is $\sim 2.8 \times 10^4$ M^{-1} in 0.15 M NaCl. This compares with a value of $\sim 2.7 \times 10^8$ for native A1 (Nadler *et al.*, 1991). On the basis of these data we calculate that the two RBDs in A1 together contribute only about 53% of the overall free energy of binding with the remaining binding energy deriving from cooperative and direct nucleic acid interactions mediated by the glycine-rich COOH-terminal domain of A1 (Nadler *et al.*, 1991).

The ease with which the two RBDs in A1 (Merrill *et al.*, 1986; Casas-Finet *et al.*, 1993) can be cleaved apart via limited proteolysis as well as dynamic anisotropy data (Casas-Finet *et al.*, 1991) strongly suggest that the two RBDs in A1 are held together with a very flexible linkage. Our finding that the circular dichroism spectra of the 1–92 and 93–184 fragments approximately sum to that of the 1–184 peptide further suggests that these two RBDs are noninteracting and are independently folded, globular domains. This conclusion is also consistent with the demonstrated resistance of these RBDs to further proteolysis (Merrill *et al.*, 1986; Casas-Finet *et al.*, 1993). It is clear from the binding studies described in this work that an individual A1 RBD has relatively low affinity for nucleic acids. On the basis of poly[r(ϵA)] and poly[d(ϵA)] binding studies, each of the A1 RBDs has an affinity at pH 8 of less than 5×10^4 M^{-1} for RNA (Table 2) and about an 8-fold (at pH 6) higher affinity for RNA as compared to DNA. Since other individual RBDs have been reported to have much higher affinities [e.g., $\sim 10^7$ M^{-1} for RBD-IV of the yeast poly(A) binding protein (Sachs *et al.*, 1987) and 10^8 M^{-1} for the U1A RBD-I:U1 RNA stem-loop II interaction (Jessen *et al.*, 1991)], we hypothesize that the A1 RBD affinity represents a "basal level" of affinity that is probably common to all RBDs. Another example of a "basal level" of RBD binding affinity is provided by the first RBD of nucleolin, where the K_{app} for nonspecific versus specific RNA targets are ca. 1×10^5 and 2×10^6 M^{-1}, respectively (Ghisolfi *et al.*, 1992). Because the "basal" level of affinity for A1 is so low, it could be easily missed by nonequilibrium assays such as filter binding studies. RBD affinity could then be increased by modifying the RBD and/or the NH_2- and COOH-terminal sequences flanking the RBDs, as suggested by several investigators (Query *et al.*, 1989; Schery *et al.*, 1989). The latter point is well illustrated by the 100-fold contribution that residues 185–195 make toward the overall affinity of A1 hnRNP for ssRNA.

Our results clearly suggest that while the 1–92 and 93–184 domains of A1 are well folded, semi-independent domains further reduction of the 1–92 domain by synthesizing peptides corresponding to residues 4–49 and 50–93 results in substantial alterations in secondary structure, as evidenced by the fact that the CD spectra of these two fragments does not sum to that of the intact 1–92 domain. In light of the structures that have been published for the homologous U1A snRNP protein (Nagai *et al.*, 1990; Hoffman *et al.*, 1991) and hnRNP C (Wittekind *et al.*, 1992; Gorlach *et al.*, 1992), it is not hard to understand why the 4–49 and 50–93 peptides are misfolded. In the U1A and hnRNP C RBD structures, four antiparallel β-sheets and two α-helices fold such that the NH_2-terminal β-sheet$_1$ is packed against α-helix$_1$, β-sheet$_3$, and β-sheet$_4$. β-Sheet$_3$ and β-sheet$_4$ both originate from the C-terminal half of the U1A (Nagai *et al.*, 1990; Hoffman *et al.*, 1991) and, hence, in the case of the 4–49 peptide would be absent. What is surprising is that despite the obviously non-native structure of the 50–93 synthetic peptide analogue, its affinity for poly[r(ϵA)] is actually greater than that of the properly folded 1–93 protein. This finding reinforces the suggestion that was made previously (Nadler *et al.*, 1992) that, unless a synthetic peptide analogue has been demonstrated to assume the same conformation as that stretch of sequence does in the parent protein, considerable caution must be exercised in interpreting results of structure/function studies on the peptide analogue.

As mentioned earlier, proteins have been found which have from one to four tandemly arranged RBDs (Dreyfuss *et al.*, 1993). In order to directly approach the question of whether or not both A1 RBDs contribute to binding we have compared the free energy of binding of the isolated RBDs with that of the intact 1–184 domain for poly[r(ϵA)]. These data (Table 2) demonstrate that the affinity of the 1–184 domain for ssRNA is substantially greater than that of either isolated domain but yet it is less than the product of the individual RBD affinities. Hence, at pH 6, the affinity of the 1–184 fragment is 24-fold higher than that of the 93–184 domain and 325-fold higher than the 1–92 domain. However, at pH 6 the observed affinity of the 1–184 domain for ssRNA is over 1000-fold less than the product of the affinities of its isolated RBDs. Therefore, although the apparent free energy of binding of the two RBDs is nonadditive, the fact that the affinity of 1–184 for poly[r(ϵA)] is more than 1 order of magnitude above that of either of its component RBD strongly suggests that both contribute toward binding. This conclusion also provides an explanation of the biphasic "reverse titration" binding isotherm for poly(U) that was observed in Figure 5 and is consistent with the increased occluded site size that was observed with 1–184 ($n = 14 \pm 2$) as compared to that for an individual RBD ($n = 6 \pm 1$). It is important to note that site sizes were determined under stoichiometric binding conditions but that even if the 93–184 binding was so weak as to be nonstoichiometric, the calculated site size from forward titrations with poly[r(ϵA)] would decrease, rather than increase, thus our determination of $n = 6 \pm 1$ for the 93–184 fragment represents a maximum size.

While other explanations are possible, we postulate that the primary reason the "apparent" affinity of the 1–184 fragment is 1000-fold less than the product of the affinities of its component RBDs is because the second interactive RBD is connected by a flexible linker to the first domain (Casas-Finet *et al.*, 1991). Crothers and Metzger (1972) have presented a general formalism for the binding of a divalent ligand that contains two independent binding domains connected by a flexible linker. As applied to the 1–184 fragment, their theory accounts for the fact that when RBD I is bound to polynucleotide, the local effective concentration of the "free"

RBD II is considerably less than that required for the affinity of the 1–184 to be simply the product of the two isolated affinities. It should be recalled that affinities are determined relative to the standard state, which is usually taken to be 1 M. In the case of the 1–184 fragment, the two RBDs are connected by a linker that might be as long as 17 amino acids which could in turn span 60 Å. If we add 30 Å to this to approximate the contribution of the radii of the two RBDs (based on a diameter of about 30 Å from the crystal structure of the homologous U1A RBD, Nagai *et al.*, 1990), then the "free" RBD could sweep out a sphere of ca. 90 Å. The latter corresponds to an effective concentration of only 0.55 mM. Using 90 Å as the mean free radius (r) of the two domains, and assuming the 93–184 RBD binds first, then from eq 16 of Crothers and Metzger (1972) we calculate the expected affinity (K_2') for the subsequent binding of the 1–92 RBD as

$$K_2' = 3V(K_2)/4\pi(r^3)N \quad (1)$$

In this equation, N equals the number of particles per volume (V) is the standard state defined for K_2, which is the affinity of 1–92 when it is not linked to 93–184 (i.e. 1.5×10^4 M^{-1}). Using the above relationship we calculate a value of only 8.2 M^{-1} for K_2'. The observed equilibrium (K_{obs}) can then be calculated from

$$K_{obs} = 2K_1(1 + K_2') \quad (2)$$

where K_1 is the affinity of the 93–184 fragment when it is not linked to 1–92 and the factor of 2 is for degeneracy arising from interchange of the two RBDs (Crothers & Metzger, 1972). The calculated K_{obs} for the two RBD system is 8.3×10^5 M^{-1}, which is within a factor of 2 of the experimentally measured value of 5.4×10^5 M^{-1} for the 1–184 fragment. The use of these considerations alone accounts for most, if not all, of the decreased affinity for binding observed for the 1–184 fragment as compared to that predicted from the product of the affinities of the individual RBDs (6.8×10^8 M^{-1}). The factor of 2 difference that remains might result from entropic and/or steric effects.

When taken together with studies on other RBD-containing proteins, our results suggest there are at least two general mechanisms by which RNA binding proteins that contain multiple RBDs interact with nucleic acids. In one instance, binding would appear to be attributable to only a single RBD. Examples of this class of interactions include the U1 snRNP-A:U1 RNA complex, where only the first of two RBDs contributes to binding (Lutz-Freyermuth *et al.*, 1990) and the nucleolin:rRNA interaction, where deletion of RBDs II→IV has no effect on binding (Ghisolfi *et al.*, 1992). In this class of RNA binding proteins the other RBDs may well have specificity for other targets. The A1 hnRNP:poly[r(ϵA)] complex would appear to represent another class of interactions where multiple RBDs contribute to binding. Other members of this class include the poly(A) binding protein:poly(A) interaction, where RBDs I and II (in this four RBD protein) are required for efficient binding (Burd *et al.*, 1991) and the U2AF:mRNA polypyrimidine tract interaction where all three RBDs in this splicing factor contribute to binding. As in the case of A1, however, the contribution of individual U2AF RBDs to binding appears to be nonadditive in that deletion of RBDs I and II (from this three RBD domain protein) decreases its affinity for two different pre-mRNA polypyrimidine tracts sequences by only about 10-fold (Zamore *et al.*, 1992). This relatively small difference in the free energy of binding (i.e., <20%) may, however, have an important function, as Zamore *et al.* (1992) found that U2AF binds more tightly to mRNAs as the length of their polypyrimidine tract increases. They suggest that the length of the polypyrimidine tract is an important determinant of the ability of U2AF to regulate splice site selection. Presumably, as the length of the polypyrimidine tract is increased, more of the individual RBD domains in U2AF can interact with the pre-mRNA, and hence, the overall affinity for U2AF is increased. In a sense, then, our observation that binding of the individual RBDs of hnRNP A1 is nonadditive is consistent with the idea that one of the functions of tandemly arranged RBDs is to allow simultaneous interactions with different RNA sequences or structures. Thus a protein containing more than one RBD may actually make either *cis* interactions along a single RNA molecule or *trans* interactions on a heterologous strand. Our results suggest that either of these modes of RNA binding could be possible for hnRNP A1, but that in either case, both RBDs within A1 are able to interact with nucleic acids in order to give A1 its high affinity for ssRNA.

ACKNOWLEDGMENT

We would like to especially thank Dr. Don Crothers for reading the manuscript and for calling attention to the significance of his earlier studies (on divalent antibody binding) to the present work.

REFERENCES

Adam, S. A., Nakagawa, T., Swanson, M. S., Woodruff, T. K., & Dreyfuss, G. (1986) *Mol. Cell. Biol. 6*, 2932–2943.
Bandziulis, R. J., Swanson, M. S., & Dreyfuss, G. (1989) *Genes Dev. 3*, 431–437.
Beyer, A. L., Christensen, M. E., Walker, B. W., & LeStourgeon, W. M. (1977) *Cell 11*, 127–138.
Biamonti, G., Bassi, M. T., Cartegna, L., Mechta, F., Buvoli, M., Cobianchi, F., & Riva, S. (1993) *J. Mol. Biol. 230*, 77–89.
Burd, C. G., Matunis, E. L., & Dreyfuss, G. (1991) *Mol. Cell. Biol. 11*, 3419–3424.
Buvoli, M., Cobianchi, F., Biamonti, G., & Riva, S. (1990) *Nucleic Acids. Res. 18*, 6595–6600.
Calnan, B. J., Biancalana, S., Hudson, D., & Frankel, A. D. (1991) *Genes Dev. 5*, 201–210.
Casas-Finet, J. R., Karpel, R. L., Maki, A. H., Kumar, A., & Wilson, S. H. (1991) *J. Mol. Biol. 221*, 693–709.
Casas-Finet, J. R., Smith, J. D., Kumar, A., Kim, J. G., Wilson, S. H., & Karpel, R. L. (1993) *J. Mol. Biol. 229*, 873–889.
Chang, J. T., Wu, C. S. C., & Yang, J. T. (1978) *Anal. Biochem. 91*, 13–31.
Choi, Y. D., Grabowski, P. J., Sharp, P. A., & Dreyfuss, G. (1986) *Science 231*, 1534–1539.
Cobianchi, F., Sen Gupta, D. N., Zmudzka, B. Z., & Wilson, S. H. (1986) *J. Biol. Chem. 261*, 3536–3543.
Cobianchi, R., Karpel, R. L., Williams, K. R., Notario, V., & Wilson, S. H. (1988) *J. Biol. Chem. 263*, 1063–1071.
Cobianchi, F., Calvo, C., Stoppini, M., Buvoli, M., & Riva, S. (1993) *Nucleic Acids Res. 21*, 949–955.
Crothers, D. M., & Metzger, H. (1972) *Immunochemistry 9*, 341–357.
Dreyfuss, G., Swanson, M. S., & Pinol-Roma, S. (1988) *Trends Biochem. Sci. 13*, 86–91.
Dreyfuss, G., Matunis, M. J., Pinol Roma, S., & Burd, C. G. (1993) *Annu. Rev. Biochem.*, Ge, H., & Manley, J. L. (1990) *Cell 62*, 25–34.
Ghisolfi, L., Kharrat, A., Joseph, G., Amalric, F., & Erard, M. (1992) *Eur. J. Biochem. 209*, 541–548.
Görlach, M., Wittekind, M., Beckman, R. A., Mueller, L., & Dreyfuss, G. (1992) *EMBO J. 11*, 3289–3295.

Harper, J. E., & Manley, J. L. (1991) *Mol. Cell. Biol. 11*, 5945–5953.
Hoffman, D. W., Query, C. C., Golden, B. L., White, S. W., & Keene, J. D. (1991) *Proc. Natl. Acad. Sci. U.S.A. 88*, 2495–2499.
Jessen, T. H., Oubridge, C., Teo, C. H., Pritchard, C., & Nagai, K. (1991) *EMBO J. 10*, 3447–3456.
Kelly, R. C., Jensen, D. E., & von Hippel, P. H. (1976) *J. Biol. Chem. 251*, 7240–7249.
Kenan, D. J., Query, C. C., & Keene, J. D. (1991) *Trends Biochem. Sci. 16*, 214–220.
Kowalczykowski, S. C., Paul, L. S., Lonberg, N., Newport, J. W., McSwiggen, J. A., & von Hippel, P. H. (1986) *Biochemistry 25*, 1226–1240.
Kumar, A., & Wilson, S. H. (1990) *Biochemistry 29*, 10717–10722.
Kumar, A., Williams, K. R., & Szer, W. (1986) *J. Biol. Chem. 261*, 11266–11273.
Kumar, A., Casas-Finet, J. R., Luneau, C. J., Karpel, R. L., Merrill, B. M., Williams, K. R., & Wilson, S. H. (1990) *J. Biol. Chem. 265*, 17094–17100.
Lutz-Freyermuth, C., Query, C. C., & Keene, J. D. (1990) *Proc. Natl. Acad. Sci. U.S.A. 87*, 6393–6397.
Mayeda, A., & Krainer, A. R. (1992) *Cell 68*, 365–375.
McGhee, J. D., & von Hippel, P. H. (1974) *J. Mol. Biol. 86*, 469–489.
McSwiggen, J. A., Bear, D. G., & von Hippel, P. H. (1988) *J. Mol. Biol. 99*, 609–622.
Merrill, B. M., & Williams, K. R. (1990) in *The Eukaryotic Nucleus, Molecular Biochemistry and Macromolecular Assemblies* (Strauss, P., & Wilson, S., Eds.) Vol. 2, pp 579–604, Telford Press, London.
Merrill, B. M., LoPresti, M. B., Stone, K. L., & Williams, K. R. (1986) *J. Biol. Chem. 261*, 878–883.
Merrill, B. M., Stone, K. L., Cobianchi, F., Wilson, S. H., & Williams, K. R. (1988) *J. Biol. Chem. 263*, 3307–3313.
Munroe, S. H., & Dong, X. F. (1992) *Proc. Natl. Acad. Sci. U.S.A. 89*, 895–899.
Nadler, S. G., Merrill, B. M., Roberts, W. J., Keating, K. M., Lisbin, M. J., Barnett, S. F., Wilson, S. H., & Williams, K. R. (1991) *Biochemistry 30*, 2968–2976.
Nadler, S. G., Kapouch, J. L., Elliot, J. I., & Williams, K. R. (1992) *J. Biol. Chem. 267*, 3750–3757.
Nagai, K., Oubridge, C., Jessen, T. H., Li, J., & Evans, P. R. (1990) *Nature 348*, 515–520.
Pinol-Roma, S., & Dreyfuss, G. (1992) *Nature 355*, 730–732.
Query, C. C., Bentley, R. C., & Keene, J. D. (1989) *Cell 57*, 89–101.
Record, M. T., Jr., Lohman, T. M., & deHaseth, P. (1976) *J. Mol. Biol. 107*, 145–158.
Sachs, A. B., Davis, R. W., & Kornberg, R. D. (1987) *Mol. Cell. Biol. 7*, 3268–3276.
Sambrook, J., Fritsch, E. F., & Maniatis, T. (1989) in *Molecular Cloning* (Nolan, C., Ed.) Cold Spring Harbor Press, Cold Spring Harbor.
Scherly, D., Boelens, W., van Vernrooij, W. J., Dathan, N. A., Hamm, J., & Mattaj, I. W. (1989) *EMBO J. 8*, 4163–4170.
Shamoo, Y., Adari, H., Konigsberg, W. H., Williams, K. R., & Chase, J. R. (1986) *Proc. Natl. Acad. Sci. U.S.A. 83*, 8844–8848.
Sierakowska, H., Szer, W., Furdon, P. J., & Role, K. (1986) *Nucleic Acids Res. 14*, 5241–5254.
Swanson, M. S., & Dreyfuss, G. (1988) *EMBO J. 11*, 3519–3529.
Valentini, O., Biamonti, G., Pandolfo, M., Morandi, C., & Riva, S. (1985) *Nucleic Acids Res. 13*, 337–346.
Williams, K. R., Stone, K. L., LoPresti, M. B., Merrill, B. M., & Planck, S. (1985) *Proc. Natl. Acad. Sci. U.S.A. 82*, 5666–5670.
Wilson, S. H., Cobianchi, F., & Guy, H. R. (1987) in *DNA, Protein interaction & Gene Regulation* (Thompson, E. B., & Papaconstatinou, J., Eds.) pp 129–146, University of Texas Press, Austin.
Wittekind, M., Görlach, M., Friedrichs, M., Dreyfuss, G., & Mueller, L. (1992) *Biochemistry 31*, 6254–6265.
Zamore, P. D., & Green, M. R. (1992) *Nature 355*, 609–614.